JACS
JOURNAL OF THE AMERICAN CHEMICAL SOCIETY
Communication
pubs.acs.org/JACS

Engineering the Optical Response of the Titanium-MIL-125 Metal–Organic Framework through Ligand Functionalization

Christopher H. Hendon,[†] Davide Tiana,[†] Marc Fontecave,[‡] Clément Sanchez,[§] Loïc D'arras,[§] Capucine Sassoye,[§] Laurence Rozes,*[,§] Caroline Mellot-Draznieks,*[,‡] and Aron Walsh*[,†]

[†]Department of Chemistry, University of Bath, Claverton Down, Bath BA2 7AY, U.K.

[‡]Laboratoire de Chimie des Processus Biologiques, Collège de France, CNRS FRE 3488, 11 Place Marcelin Berthelot, 75005 Paris, France

[§]UPMC Univ Paris 06, UMR 7574, Chimie de la Matière Condensée de Paris, Collège de France, 11 Place Marcelin Berthelot, 75231 Paris Cedex 05, France

Supporting Information

ABSTRACT: Herein we discuss band gap modification of MIL-125, a TiO_2/1,4-benzenedicarboxylate (**bdc**) metal–organic framework (MOF). Through a combination of synthesis and computation, we elucidated the electronic structure of MIL-125 with aminated linkers. The band gap decrease observed when the monoaminated **bdc-NH_2** linker was used arises from donation of the N 2p electrons to the aromatic linking unit, resulting in a red-shifted band above the valence-band edge of MIL-125. We further explored in silico MIL-125 with the diaminated linker **bdc-$(NH_2)_2$** and other functional groups (−OH, $-CH_3$, −Cl) as alternative substitutions to control the optical response. The **bdc-$(NH_2)_2$** linking unit was predicted to lower the band gap of MIL-125 to 1.28 eV, and this was confirmed through the targeted synthesis of the **bdc-$(NH_2)_2$**-based MIL-125. This study illustrates the possibility of tuning the optical response of MOFs through rational functionalization of the linking unit, and the strength of combined synthetic/computational approaches for targeting functionalized hybrid materials.

Metal–organic frameworks (MOFs) are a class of structures composed of organic and inorganic building blocks. These highly ordered and porous networks are of interest for their applications in gas storage, catalysis, and photoelectrics.[1−10] In particular, MOFs have the ability to behave as semiconductors when exposed to light,[11,12] making them unique platforms for light harvesting and photoinduced catalysis.[13] A subfield of research has thus emerged with the aim of tuning the optical response of MOFs by modifying the inorganic unit or the organic linker (length, chemical functionalization) through synthetic[14,15] or computational screening.[16−22] In this context, the highly porous titanium-based MOF MIL-125 (MIL = Materials of Institut Lavoisier) (Figure 1) is an interesting candidate.[23] This material, which contains cyclic octamers of TiO_2 octahedra, is photochromic, which is related to the reduction of Ti(IV) to Ti(III) under UV irradiation.[24]

When synthesized with the 1,4-benzenedicarboxylate (**bdc**) linker, MIL-125 has an optical band gap in the UV region (ca. 3.6 eV/345 nm; see Figure 3a) and is an active photocatalyst for the oxidation of alcohols to aldehydes.[23] MIL-125-**NH_2** made with the monoaminated **bdc-NH_2** linker[25] was reported to be a photocatalyst with visible-light-induced activity for CO_2 reduction[26] and H_2 production.[27] The **bdc-NH_2** linker was shown to be responsible for the extra absorption band in the visible region, indicative of a band gap reduction (to ca. 2.6 eV/475 nm).[25−28] García and co-workers further confirmed the ability of MIL-125-**NH_2** to undergo photoinduced charge separation.[29] A similar band gap reduction and red shift were reported for Zr-UiO-66 upon synthesis with **bdc-NH_2**, emphasizing the electronic role of the $-NH_2$ group in determining the optical response in MOFs.[30] Coincidently, aminated linkers are becoming particularly popular in porous MOF synthesis, as polar $-NH_2$ groups are expected to enhance CO_2 capture, yield selective gas adsorption,[31−35] and enable postsynthetic modifications.[36−38]

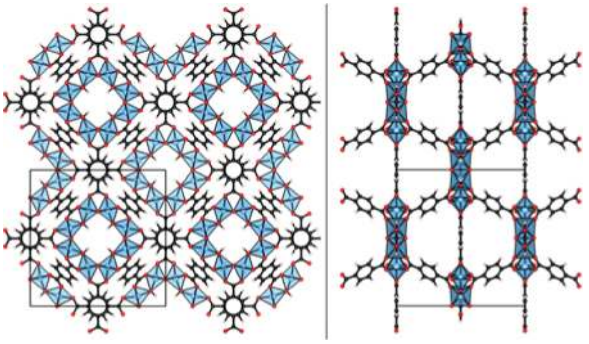

Figure 1. (left) [001] and (right) [010] orientations of MIL-125. Ti, O, C, and H are depicted in blue, red, black, and beige, respectively.

These recent findings make it necessary to develop strategies to control the band gap of MIL-125. Here we performed a combined experimental and computational study to elucidate the band structure of MIL-125 and the impact of functional groups on the **bdc** linker, exploring the observed red shift in MIL-125-**NH_2**. We then computationally predicted the beneficial impact of using the diaminated **bdc-$(NH_2)_2$** linker, which was confirmed by a targeted synthesis. We finally explored in silico other

Received: May 28, 2013
Published: July 10, 2013

potential **bdc** linkers (Figure 2) as candidates for optical control in MIL-125.

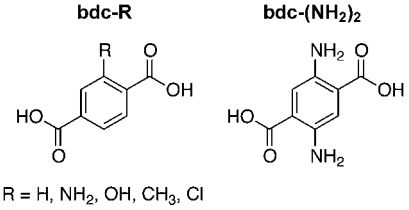

Figure 2. Neutral linking molecules explored in this study: (left) monosubstituted linkers **bdc-R**; (right) diaminated linker **bdc-$(NH_2)_2$**.

Amines are ring-activating substituents; as an initial study, we investigated the change in the band gap in response to increasing the concentration of monoaminated **bdc-NH_2**. MIL-125 (Figure 3a) and three aminated MIL-125 analogues (Figure 3b–d) were synthesized under solvothermal conditions by varying the ratio of **bdc** and **bdc-NH_2** linkers (i.e., 10%, 50%, and 100% **bdc-NH_2**, equating to ~1, 6, and 12 **bdc-NH_2** linkers per unit cell). Figure 3 presents scanning electron microscopy (SEM) images of these four samples and their accompanying UV spectra and powder colors. It is apparent that the absorption onset (ca. 475 nm) is similar for all of the monoaminated samples. The samples also demonstrated similar band gaps of ~2.6 eV [Table S2 in the Supporting Information (SI)], but the molar extinction coefficient notably increased in proportion with the **bdc-NH_2** content. This feature was reflected in the physical crystal appearance: the yellow color increased in intensity. This characteristic absorption pattern suggests that a single $-NH_2$ motif is responsible for the reduced band gap of the monoaminated series of MIL-125 analogues.

Electronic structure calculations on the same series of monoaminated MIL-125-**NH_2** solids were performed using density functional theory (DFT) as described in the SI. Figure 4a,b depicts the valence band (VB) and conduction band (CB) orbitals, respectively, for standard MIL-125. The upper VB is composed of **bdc** aromatic 2p orbitals. Introducing a single **bdc-NH_2** linker per unit cell (i.e., to give 10%-MIL-125-**NH_2**) breaks the original *I*4/*mmm* symmetry and splits the VB into a high-energy occupied state (depicted in blue in Figure 4c). The other aromatic bands are also split within 0.3 eV of each other and contribute to the VB-1,2...12. Because of the strong electron-donating characteristics of aromatic amines, the modified VB is 1.2 eV above that of MIL-125 (depicted with the blue arrow in Figure 4c), resulting in the lower band gap. This localized electronic modification results in a flat band in **k** space, which emphasizes the absence of long-range chemical interactions.

Further calculations were carried out by systematically increasing the amine content from 1 to 12 **bdc-NH_2** linkers per unit cell (Figure 4d). It is apparent that the VB is modified upon amination of the linker while the lower CB is unchanged. Thus, a single $-NH_2$ group electronically saturates MIL-125. The band structure of 10%-MIL-125-**NH_2** (blue in Figure 4c) depicts a localized noninteracting state, which was observed for all of the monoaminated systems independent of the **bdc-NH_2** content.

The amine functional motif plays a crucial role in the band structure of MIL-125. We therefore considered the plausible extension of further increasing the electron density of the aromatic motifs through polyamination of the **bdc** linker. Selecting diaminated **bdc-$(NH_2)_2$** (Figure 2 right) as a potentially interesting linker, we constructed a 10%-MIL-125-**$(NH_2)_2$** model as a mixture of 10% **bdc-$(NH_2)_2$** and 90% **bdc** and computed its band structure (shown in green in Figure 4c). This model may be compared to its monoaminated analogue (shown in blue in Figure 4c). Our calculations predicted that 10%-MIL-125-**$(NH_2)_2$** would exhibit a larger red shift due to the increase in aromatic electronic density, with a resultant band gap of 1.28 eV.

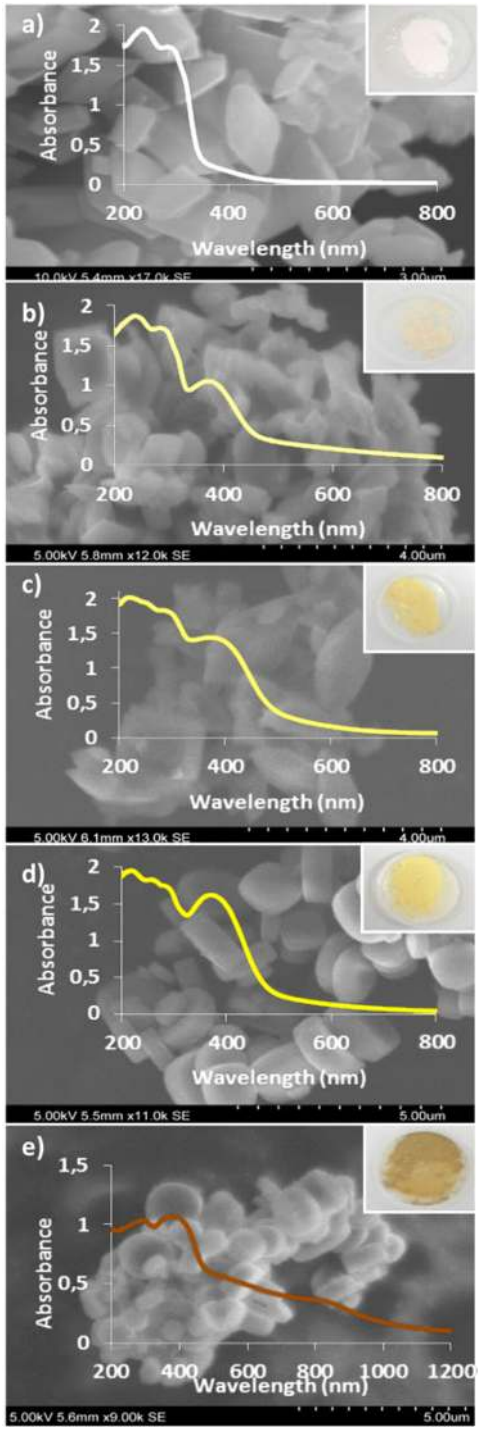

Figure 3. SEM images of (a) MIL-125, (b) 10%-MIL-125-**NH_2**, (c) 50%-MIL-125-**NH_2**, (d) 100%-MIL-125-**NH_2**, and (e) 10%-MIL-125-**$(NH_2)_2$**/90%-MIL-125-**NH_2**, with their respective UV spectra and powder colors. All of the monoaminated systems show the same absorption onset.

dx.doi.org/10.1021/ja405350u | *J. Am. Chem. Soc.* 2013, 135, 10942–10945

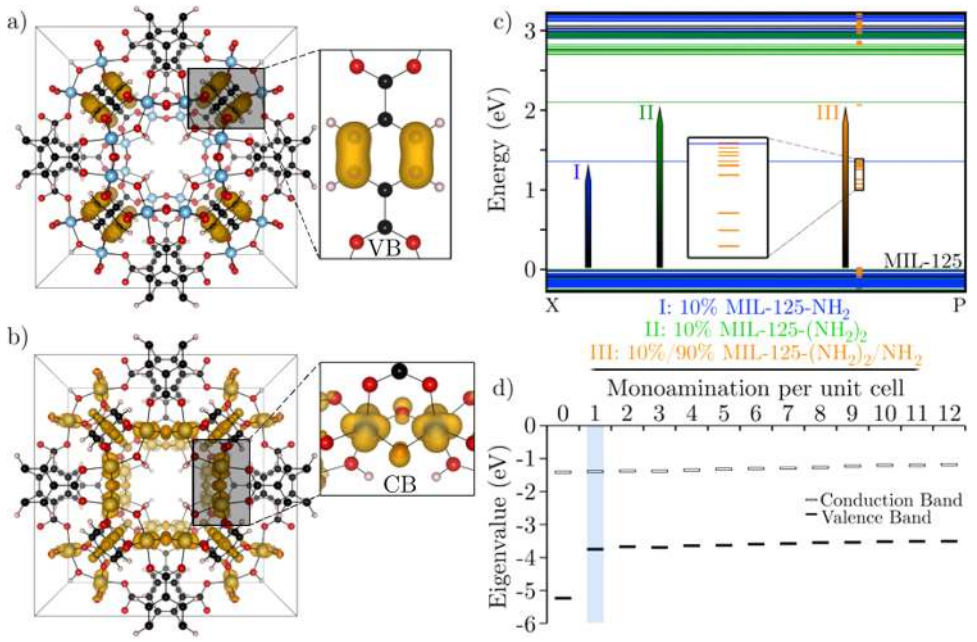

Figure 4. (a, b) Frontier electron density of unsubstituted MIL-125: (a) the valence band is composed of the **bdc** C 2p orbitals (shown on the right), making these favorable for linker-based band gap modifications; (b) the conduction band is composed of O 2p orbitals and Ti 3d orbitals (shown on the right), suggesting that modifications of the aromatic **bdc** units are unlikely to affect the CB. Isovalue = 0.001 e·Å^{-3}. (c) PBEsol band structures for synthetic MIL-125 (black), 10%-MIL-125-$\mathbf{NH_2}$ (blue), 10%-MIL-125-$\mathbf{(NH_2)_2}$/90%-MIL-125-$\mathbf{NH_2}$ (orange) and the theoretical 10%-MIL-125-$\mathbf{(NH_2)_2}$ (green). The orange bands, which have been truncated to improve the clarity of the band structures, maintain flat characteristics. The enlarged section emphasizes the VB-1...12 of the 11 nondegenerate monoamine bands. The energies are adjusted such that the highest occupied non-amine band is at 0 eV. The changes in the occupied VBs are depicted by the arrows. PBEsol is a qualitative approach; band structures could not be computed at the HSE06 level of theory because of the system size. (d) HSE06-calculated VB and CB energies of MIL-125-$\mathbf{NH_2}$ models containing increasing numbers of **bdc**-$\mathbf{NH_2}$ linkers [i.e. 0 (MIL-125) to 12 (100%-MIL-125-$\mathbf{NH_2}$)] per unit cell. The degree of amination does not affect the band gap.

This presents a further band gap decrease of 1.1 eV relative to the 10%-monoaminated analogue.

We subsequently targeted the synthesis of a diaminated MIL-125 derivative, which was successfully achieved with a mixture of 10% **bdc**-$\mathbf{(NH_2)_2}$ and 90% **bdc**-$\mathbf{NH_2}$ (Figure 3e). This compound differs from the 10%-MIL-125-$\mathbf{(NH_2)_2}$ model described in the previous paragraph by the presence of **bdc**-$\mathbf{NH_2}$ instead of **bdc**. We did not isolate the 10%-MIL-125-$\mathbf{(NH_2)_2}$, but our compound should act electronically in a similar fashion, since the amine motifs are indeed noninteracting and produce highly localized electronic bands. Optical measurements (Figure 3e) revealed a further band gap decrease of 1.1 eV for this solid relative to the monoaminated samples to give an optical band gap of 1.3 eV, shifting the absorption onset to the red/IR region. This is in striking agreement with the above computational prediction. To approximate the blended solid, we further computed the electronic structure of a mixed 10%-MIL-125-$\mathbf{(NH_2)_2}$/90%-MIL-125-$\mathbf{NH_2}$ model (shown in Figure 4c in orange). In both the experimental spectrum and the band structure calculations we observed the presence of the monoamine motifs. The multiple orange bands in the 1−1.5 eV region are the result of the inequivalent monoamines. Our computational approach predicted a band gap of 1.55 eV (orange in Figure 5). The difference between the experimental (1.3 eV) and computed (1.55 eV) band gaps is attributed to the challenge of describing this partially disordered system computationally, including using lattice constants fixed at the equilibrium values of the parent MIL-125 structure.

Finally, we extended the computational exploration to three potential MIL-125 analogues. Amines are one of the stronger electron-donating substituents; weaker electron-donating substituents should reduce the band gap to a lesser extent.[39,40] The introduction of 10% **bdc-R** (R = −OH, −CH_3, −Cl; Figure 2 left) per unit cell resulted in flexible band gap control between 3.5 and 2.4 eV (Figure 5). The weakest electron-donating group, −CH_3, moderately decreases the band gap to 3.5 eV. Aromatic halides are more chemically complex and may be either weakly electron-donating or -withdrawing. In MIL-125, −Cl acts as a weak electron donor with a predicted band gap similar to that for the −CH_3 group. The −OH group is more electron-donating than −CH_3 and −Cl, which is reflected by the predicted band gap of 2.8 eV for the 10%-MIL-125-**OH** model. The −Br and −CF_3 substituents were also computed. Our results suggest that −Br motifs produce band gap control similar to −Cl, but the crystal could not be stabilized above eight substitutions per unit cell. The −CF_3 group is strongly electron-withdrawing, potentially

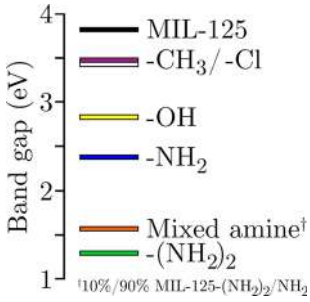

Figure 5. HSE06-predicted band gaps of MIL-125 (black) and its analogues containing functionalized **bdc** linkers. Substitutions of ca. 10% (i.e., one functionalized linker per unit cell) were made, unless otherwise stated. Control of the band gap was achieved by varying the substituent.

dx.doi.org/10.1021/ja405350u | J. Am. Chem. Soc. 2013, 135, 10942−10945

lowering a CB+*n* band into the band gap. It was found that the inclusion of $-CF_3$ resulted in destabilization of the Ti−O bond, and a single substitution produced an unstable crystal. Thus, $-NH_2$, −OH, $-CH_3$, and −Cl are the most promising and favorable substitutions.

In conclusion, we have elucidated the specific role of the $-NH_2$ group of the monoaminated **bdc-NH$_2$** linker in lowering the optical band gap of the titanium-containing MIL-125-**NH$_2$** (ca. 2.6 eV). We confirmed that electronic modifications of the aromatic motifs are localized and directly control the optical properties through modification of the valence band. DFT calculations showed that the optical response of MIL-125 may be tailored toward absorption in the visible region through rational selection of substituents of the aromatic **bdc** linker. The diaminated **bdc-(NH$_2$)$_2$** linker was expected to demonstrate the most significant red shift. This prediction was confirmed by the synthesis of 10%-MIL-125-**(NH$_2$)$_2$**/90%-MIL-125-**NH$_2$** (1.3 eV/950 nm). From the experimental perspective, we have described the synthesis of a MIL-125 derivative with mixed aminated linkers. This methodology can be further extended to the large range of aromatic linkers used in MOF synthesis, which should enable accurate and predictable band gap control in tailored frameworks. For example, the Zn−**bdc**-based IRMOF-1[14,41] has an electronic structure comparable to that of MIL-125 (3.57 eV),[39] thus posing potential for similar control of its band gap through the modifications proposed here.

■ ASSOCIATED CONTENT

Supporting Information

Synthetic procedures; PXRD, N_2 sorption, and optical band gap data; and computational details. This material is available free of charge via the Internet at http://pubs.acs.org.

■ AUTHOR INFORMATION

Corresponding Author

laurence.rozes@upmc.fr; caroline.mellot-draznieks@college-de-france.fr; a.walsh@bath.ac.uk

Notes

The authors declare no competing financial interest.

■ ACKNOWLEDGMENTS

A.W. was supported a Royal Society University Research Fellowship, while C.H.H. and D.T. were funded under an ERC Starting Grant. The work benefited from the University of Bath's High Performance Computing Facility and access to the HECToR supercomputer through membership of the U.K.'s HPC Materials Chemistry Consortium, which is funded by the EPSRC (Grant EP/F067496).

■ REFERENCES

(1) Park, J.; Wang, Z. U.; Sun, L.-B.; Chen, Y.-P.; Zhou, H.-C. *J. Am. Chem. Soc.* **2012**, *134*, 20110.
(2) Roberts, J. M.; Fini, B. M.; Sarjeant, A. A.; Farha, O. K.; Hupp, J. T.; Scheidt, K. A. *J. Am. Chem. Soc.* **2012**, *134*, 3334.
(3) Martin, R. L.; Haranczyk, M. *Chem. Sci.* **2013**, *4*, 1781.
(4) Thematic issue on MOFs: *Chem. Rev.* **2012**, *112*, 673−1268.
(5) Li, J.-R.; Kuppler, R. J.; Zhou, H.-C. *Chem. Soc. Rev.* **2009**, *38*, 1477.
(6) Allendorf, M. D.; Schwartzberg, A.; Stavila, V.; Talin, A. A. *Chem.—Eur. J.* **2011**, *17*, 11372.
(7) Farrusseng, D.; Aguado, S.; Pinel, C. *Angew. Chem., Int. Ed.* **2009**, *48*, 7502.
(8) Ma, L.; Abney, C.; Lin, W. *Chem. Soc. Rev.* **2009**, *38*, 1248.
(9) Corma, A.; García, H.; Llabrés i Xamena, F. X. *Chem. Rev.* **2010**, *110*, 4606.
(10) Banerjee, R.; Phan, A.; Wang, B.; Knobler, C.; Furukawa, H.; O'Keeffe, M.; Yaghi, O. M. *Science* **2008**, *319*, 939.
(11) Alvaro, M.; Carbonell, E.; Ferrer, B.; Llabrés i Xamena, F. X.; García, H. *Chem.—Eur. J.* **2007**, *13*, 5106.
(12) Silva, C. G.; Corma, A.; García, H. *J. Mater. Chem.* **2010**, *20*, 3141.
(13) Wang, J.-L.; Wang, C.; Lin, W. *ACS Catal.* **2012**, *2*, 2630.
(14) Gascon, J.; Hernández-Alonso, M. D.; Almeida, A. R.; van Klink, G. P. M.; Kapteijn, F.; Mul, G. *ChemSusChem* **2008**, *1*, 981.
(15) Lin, C.-K.; Zhao, D.; Gao, W.-Y.; Yang, Z.; Ye, J.; Xu, T.; Ge, Q.; Ma, S.; Liu, D.-J. *Inorg. Chem.* **2012**, *51*, 9039.
(16) Fuentes-Cabrera, M.; Nicholson, D. M.; Sumpter, B. G.; Widom, M. *J. Chem. Phys.* **2005**, *123*, No. 124713.
(17) Choi, J. H.; Choi, Y. J.; Lee, J. W.; Shin, W. H.; Kang, J. K. *Phys. Chem. Chem. Phys.* **2009**, *11*, 628.
(18) Kuc, A.; Enyashin, A.; Seifert, G. *J. Phys. Chem. B* **2007**, *111*, 8179.
(19) Yang, L.-M.; Ravindran, P.; Vajeeston, P.; Tilset, M. *RSC Adv.* **2012**, *2*, 1618.
(20) Yang, L.-M.; Ravindran, P.; Vajeeston, P.; Tilset, M. *J. Mater. Chem.* **2012**, *22*, 16324.
(21) Choi, J. H.; Jeon, H. J.; Choi, K. M.; Kang, J. K. *J. Mater. Chem.* **2012**, *22*, 10144.
(22) Hendon, C. H.; Tiana, D.; Vaid, T. P.; Walsh, A. *J. Mater. Chem. C* **2013**, *1*, 95.
(23) Dan-Hardi, M.; Serre, C.; Frot, T.; Rozes, L.; Maurin, G.; Sanchez, C.; Férey, G. *J. Am. Chem. Soc.* **2009**, *131*, 10857.
(24) Walsh, A.; Catlow, C. R. A. *ChemPhysChem* **2010**, *11*, 2341.
(25) Zlotea, C.; Phanon, D.; Mazaj, M.; Heurtaux, D.; Guillerm, V.; Serre, C.; Horcajada, P.; Devic, T.; Magnier, E.; Cuevas, F.; Férey, G.; Llewellyn, P. L.; Latroche, M. *Dalton Trans.* **2011**, *40*, 4879.
(26) Fu, Y.; Sun, D.; Chen, Y.; Huang, R.; Ding, Z.; Fu, X.; Li, Z. *Angew. Chem. Int. Ed.* **2012**, *51*, 3364−3367.
(27) Horiuchi, Y.; Toyao, T.; Saito, M.; Mochizuki, K.; Iwata, M.; Higashimura, H.; Anpo, M.; Matsuoka, M. *J. Phys. Chem. C* **2012**, *116*, 20848.
(28) Kim, S.-N.; Kim, J.; Kim, H.-Y.; Cho, H.-Y.; Ahn, W.-S. *Catal. Today* **2013**, *204*, 85.
(29) de Miguel, M.; Ragon, F.; Devic, T.; Serre, C.; Horcajada, P.; García, H. *ChemPhysChem* **2012**, *13*, 3651.
(30) Long, J.; Wang, S.; Ding, Z.; Wang, S.; Zhou, Y.; Huang, L.; Wang, X. *Chem. Commun.* **2012**, *48*, 11656.
(31) Devic, T.; Horcajada, P.; Serre, C.; Salles, F.; Maurin, G.; Moulin, B.; Heurtaux, D.; Clet, G.; Vimont, A.; Grenéche, J.-M.; Le Ouay, B.; Moreau, F.; Magnier, E.; Filinchuk, Y.; Marrot, J.; Lavalley, J.-C.; Daturi, M.; Férey, G. *J. Am. Chem. Soc.* **2010**, *132*, 1127.
(32) Torrisi, A.; Mellot-Draznieks, C.; Bell, R. G. *J. Chem. Phys.* **2010**, *132*, No. 044705.
(33) Torrisi, A.; Bell, R. G.; Mellot-Draznieks, C. *Cryst. Growth Des.* **2010**, *10*, 2839.
(34) Couck, S.; Denayer, J. F. M.; Baron, G. V.; Rémy, T.; Gascon, J.; Kapteijn, F. *J. Am. Chem. Soc.* **2009**, *131*, 6326.
(35) Wang, X.; Li, H.; Hou, X.-J. *J. Phys. Chem. C* **2012**, *116*, 19814.
(36) Jiang, D.; Keenan, L. L.; Burrows, A. D.; Edler, K. J. *Chem. Commun.* **2012**, *48*, 12053.
(37) Politzer, P.; Abrahmsen, L.; Sjoberg, P. *J. Am. Chem. Soc.* **1984**, *106*, 855.
(38) Cohen, S. M. *Chem. Rev.* **2012**, *112*, 970.
(39) Hendon, C. H.; Tiana, D.; Walsh, A. *Phys. Chem. Chem. Phys.* **2012**, *14*, 13120.
(40) Bunnett, J. F.; Morath, R. J.; Okamoto, T. *J. Am. Chem. Soc.* **1955**, *77*, 5055.
(41) Tranchemontagne, D. J.; Hunt, J. R.; Yaghi, O. M. *Tetrahedron* **2008**, *64*, 8553.

■ NOTE ADDED AFTER ASAP PUBLICATION

Reference 26 was replaced on July 16, 2013.